Consiglio Nazionale delle Ricerche

Istituto di Scienze dell'Atmosfera e del Clima — CNR ISAC

Technical report
ATMO-ACCESS TNA-5G-000000091 at ÉVora Atmospheric Sciences Observatory (EVASO) of the University of Évora

Relationship between ground-based microwave integrated WAter Vapor and satellite prEcipitation intensity at the Evora Atmospheric Science Observatory (WAVE)

Sante Laviola and Elsa Cattani
National Research Council of Italy (CNR)
Institute of Atmospheric Sciences and Climate (ISAC) – Bologna, Italy

June 2025

1. Objective of the study
2. Experimental method and work plan
3. Data and methods
4. Results
5. Conclusions and potential impacts

References
Acknowledgments

1. Objective of the study

Water vapor is a key element of water cycle and is essential for human life. Accurate observations of water vapor amount and its spatial and temporal variations are extremely important to evaluate radiation budget at global scale, considering that it is the most important greenhouse gas in the atmosphere, and the effects of rainfall on human activities. In fact, atmospheric water vapor is one of the key factors driving extreme precipitation events causing flash floods, soil erosion, and urban waterlogging.

The Global Precipitation Measurement (GPM) (Hou et al., 1014) is an international satellite mission designed to unify and advance precipitation estimates from research and operational microwave sensors. The GPM Core Observatory carrying an advanced combined active/passive microwave sensor package (i.e., GPM Microwave Imager – GMI, Dual Polarization Radar – DPR) has established new reference standards for precipitation assessment from space. In addition to the Core Observatory, the GPM satellite constellation (GPM-C) currently includes several types of passive microwave (PMW) radiometers. The high correlation between precipitation intensity and brightness temperatures (BT) measured from PMW sensors has been largely used as a diagnostic basis for identifying rain clouds and deriving hydrometeor phase. The Water vapour Strong Lines at 183 GHz (183-WSL) algorithm, developed by Laviola et al. (2011; 2013), is a fast retrieval method used to infer precipitation rates by exploiting the water vapor absorption frequencies at 183.31 GHz on board the GPM-C sensors at their native space-time resolution.

This project aims to study the space-time relationship between the integrated water vapor (IWV) provided by the ERA-5 reanalysis and the ground-based MW radiometer (MWR) (RPG Humidity And Temperature PROfiler - HATPRO) installed at the Évora Atmospheric Sciences Observatory (EVASO) of the University of Évora and the precipitation rates derived by the183-WSL method applied to GPM-C observations. MWRs are known to overestimate water vapor measurements under intense precipitation (Vaquero-Martínez et al., 2023), therefore the scientific goal of the project is improving the knowledge on IWV variations before and after precipitation events by evaluating the changes of IWV values as a function of precipitation intensity and type, convective and stratiform, inferred by the 183-WSL algorithm. Rain gauge measurements available at EVASO and ERA-5 reanalysis are used to define the duration of rain events. The project counted on the collaboration of Maria João Costa and Daniele Bortoli (both Professors at the University of Évora), experts in optical remote sensing and ground based MWR products. The HATPRO installed at EVASO measures the sky brightness temperature at different elevation angles, in the bands from 22 to 31 GHz and 51 to 58 GHz, with a radiometric accuracy between 0.3 and 0.4 K root mean square error at 1.0 s integration time. The IWV is obtained using a neural network approach with the brightness temperatures as input.

2. Experimental method and work plan

The MWR is an efficient instrument for remotely sensing atmospheric temperature and humidity profiles as well as IWV and path-integrated cloud liquid water content (LWP) (Rose et al., 2005). A catalogue of precipitating events occurring on the domain covered by the MWR is compiled considering the output of 183-WSL algorithm applied to the GPM-C observations. The GPM-C observations and MWR measurements start from 2014 guaranteeing a consistent number of rain events. For each selected event the MWR integrated humidity profiles (IWV) is hourly averaged to evaluate the variation of WV by approaching the rain event. Different types of rain events are considered in terms of precipitation intensity and type (convective and stratiform). Thus, the distribution of daily water vapor is analyzed to find noticeable water vapor oscillations by approaching rain events.

A key phase of this project was the training at the University of Évora, focused on ground based MWR measurements and inversion algorithms used to derive water vapor products. The work plan was distributed through three Work Packages (WP):

- **WP1: precipitation events catalogue**

The CNR-ISAC and EVASO Teams collected a properly dataset to build a matchup dataset. The main condition was the availability of data from the raingauge, ground-based microwave radiometer HATPRO and 183-WSL rain rate retrievals. Other ancillary data were used to support the investigation and reinforce results.

- **WP2: visit the EVASO facility, training on MWR and acquisition of LWP/IWV data**

The CNR-ISAC Research Team gained a high-level training on the capability of the ground-based microwave radiometer HATPRO, the fundamentals of instrument functioning, maintenance in terms of cleaning the membrane covering the casing of the antenna, and liquid-O_2 periodic calibration. Then, the physical basis of the retrieval method to infer the temperature profile, the Liquid Water Path (LWP), and the Integrated Water Vapor (IWV) were introduced. Finally, EVASO Teams proposed a short introduction on the software and data format.

- **WP3: analysis of the combined IWV and precipitation data**

The results of this WP suggested to make further investigations in order to highlight the relationship between the accumulation rate of columnar water vapor in atmosphere and the begin of precipitation. This issue is particularly important for studying the precipitation regimes at local scale in frame of global warming. Because precipitation comes mainly from weather systems that feed on the water vapour stored in the atmosphere, this has generally increased precipitation intensity and the risk of heavy rain (Trenberth et al., 2007). Consequently, concentrated flash floodings and damaging runoff can be increasingly registered.

3. Methods and data

The fast retrieval method Water vapour Strong Lines at 183 GHz (183-WSL) proposed by Laviola et al. (2011; 2013) retrieves rain rates and classifies precipitation types for applications in nowcasting and weather monitoring. The retrieval scheme consists of two algorithms, over land and over ocean, that use the water vapour absorption lines at 183.31 GHz corresponding to the channels 3 (183.31±1 GHz), 4 (183.31±3 GHz) and 5 (183.31±7 GHz) of the Advanced Microwave Sounding Unit module B (AMSU-B) and of the Microwave Humidity Sounder (MHS) flying on NOAA-15-18 and Metop-A satellite series, respectively. The new release of method extends the 183-WSL capability to the Advanced Technology Microwave Sounder (ATMS) and new experiments are ongoing to cover the whole GPM constellation (GPM-C).

Recent studies allowed to improve the 183-WSL computational scheme with a novel probability-based method to identify hail clusters into the storms. The MicroWave Cloud Classification-Hail (MWCC-H) described in Laviola et al. (2020a-b) exploits the properties of the high frequency channels to classify the cloud type (stratiform/convective) by estimating the cloud top altitude and the hydrometeor phase. When a convective cloud is identified, a logistic model is used to attribute the scattering signal registered by the satellite to the presence of hailstones. It is well-know that the extinction of microwave radiation due to the hailstones is strictly related to the average particle cross-section of hail bulk. The model MWCC-H classifies hail clouds trough 4 severity-based category: hail potential (HP), hail initiation (HI), hail (H, diameters ranging from 2 to 10 cm) and super hail (SH, diameters > 10 cm).

In this study the algorithms 183-WSL and MWCC-H run together to reconstruct the instantaneous precipitation rates and identify the hail probability geolocated with the ground-based microwave radiometer HATPRO and raingauge station installed at EVASO. Hourly data of Total Column Water Vapor (TCWV) from the ECMWF ERA5 are used to improve the investigation and reinforce the results. Case studies are selected following the criterion of the complete matchup of all available data. Therefore, the whole MWR HATPRO dataset 2023-2024 was firstly filtered with raingauge measurements to isolate days with hourly precipitation higher than 0 mm. The filtering procedure identifies 61 events of precipitation. The second step of the selection procedure was checking the availability of the ground-based microwave radiometer HATPRO useful to derive the Liquid Water Path (LWP) and Integrated Water Vapor (IWV) during the rain events. Finally, the time coincident GPM-C overpasses were identified. At the end, the filtering procedure selected 5 events where all instruments both at ground and from space were available on the EVASO site.
Table 1 displays for the five precipitating events the hourly rain maxima, LWP and IWV registered from the raingauge station and the ground-based microwave radiometer HATPRO, respectively.

Date	Max Rain ($mmhr^{-1}$)	Max LWP (kgm^{-2})	Max IWV (kgm^{-2})
01 January 2023	19.70 (1800 UTC)	1.29 (h. 19)	57.38 (h. 19)
02 September 2023	17.51 (1800 UTC)	1.52 (h. 18)	57.33 (h. 19)
16 September 2023	2.98 (1600 UTC)	1.41 (h. 15)	57.34 (h. 15)
19 October 2023	14.92 (1300 UTC)	1.72 (h. 12)	57.40 (h. 13)
19 January 2024	12.736 (0800 UTC)	/	/

Table 1 - List of precipitating events registered from the raingauge station and coincident in time with the GPM-C overflies. Liquid Water Path and Integrated Water Vapor are retrieved from the ground-based microwave radiometer HATPRO. For rain event on 19 January 2024 the microwave radiometer HATPRO is missed.

4. Results

In this section the rain rates inferred by the algorithm 183-WSL are compared with other products. The aim of this comparison is understanding the distribution of rain proxy such as TCWV and LWP before the precipitation to quantify the possible increasing of atmospheric humidity as a sign of preparation to rainfall.
Fig. 1 displays the 183-WSL rain maps; the location of EVASO site is indicated with a black dot. As noted, only few events fully cover EVASO site, while in most cases very low rain rates reach the site resulting in large deviations with respect to rainfall measured from the raingauge. In fact, although such events can reach intensity higher than 15 mmh^{-1} the precipitation maximum is often located far from the EVASO site. Therefore, ground measurements can differ largely from the precipitation retrieval from space.

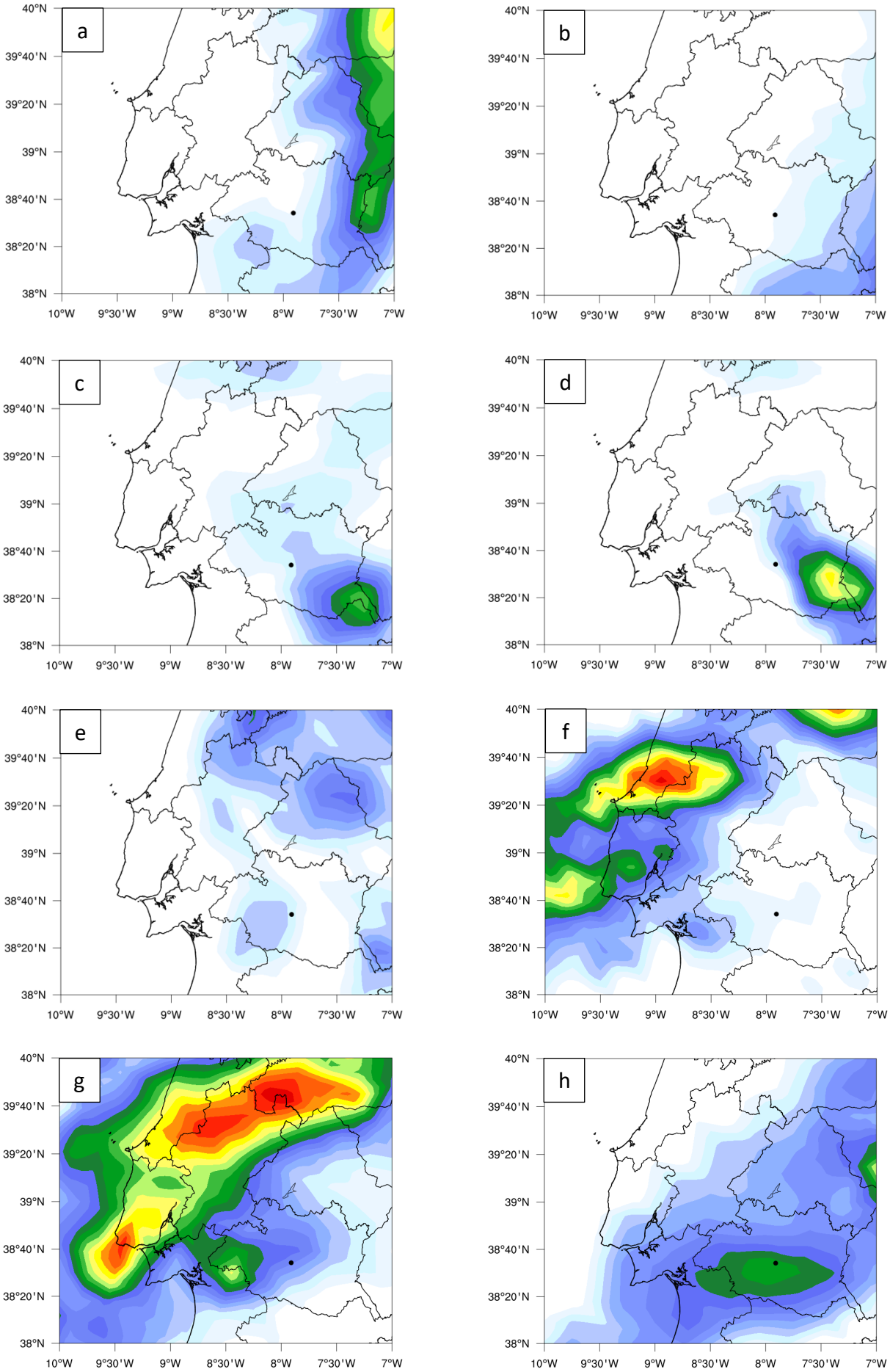
a
b
c
d
e
f
g
h
40°N
39°40'N
39°20'N
39°N
38°40'N
38°20'N
38°N
10°W
9°30'W
9°W
8°30'W
8°W
7°30'W
7°W

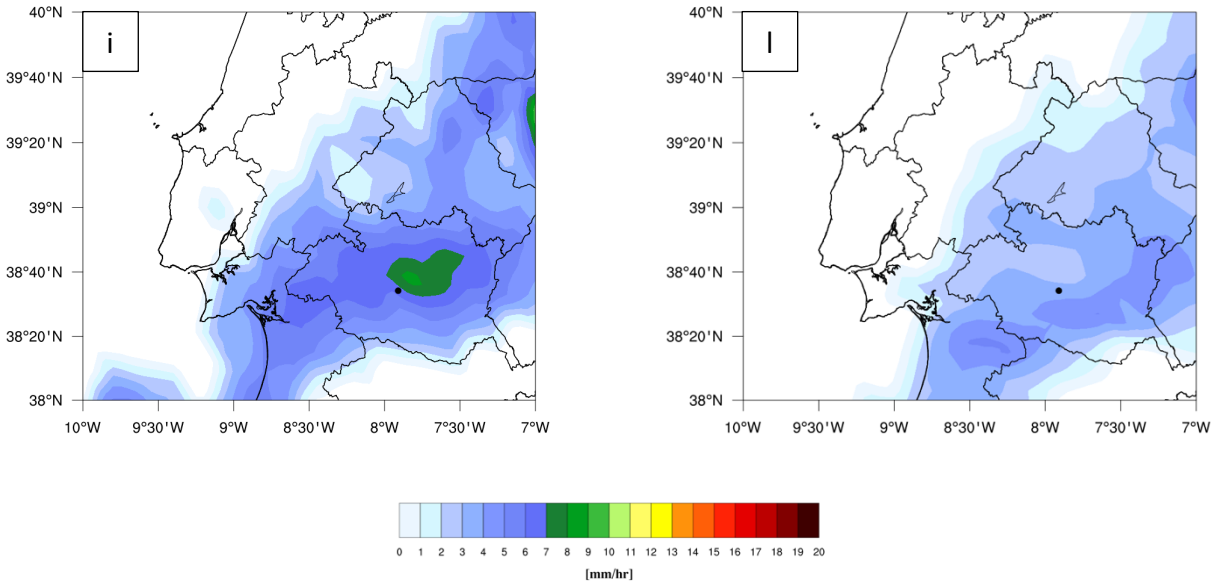

Fig. 1 – Rain rate retrievals from the 183-WSL for the case studies listed in Table 1. (a, b) 01 January 2023 at 1934 UTC and 2047 UTC, (c, d) 02 September 2023 at 2045 UTC and 2139 UTC, (e) 16 September 2023, (f, g) 19 October 2023 at 1010 UTC and 1048 UTC, (h, i, l) 19 January 2024 at 0951 UTC, 0957 UTC and 1045 UTC, respectively.

An exhaustive treatment is presented in Fig. 2 where bar diagrams delineate the distribution of hourly raingauge measurements, whereas the blue line represents the IWV derived from the microwave radiometer HATPRO and red dot the rain rates calculated from the 183-WSL algorithm. Being the IWV and precipitation rates closely linked as general consideration ought to be said that IWV fluctuates in a short range of values before rain. In fact, for clear-sky conditions the IWV shows small fluctuations around values 20-40 kgm^{-2} (see Fig. 2-a, b, c) showing in turn the tendency to accumulate humidity before starting rain. Few hours before rainfall the IWV increases making a local reservoir of humidity to feed the precipitation. Thus, IWV reaches the maximum value of 60 kgm^{-2} when the precipitation regime reaches the peak 19.70 mmh^{-1} and 17.51 mmh^{-1}, as shown in Fig. 2a and Fig.2b, respectively. From Fig. 2c and 2d a different behaviour can be noted. Being precipitation distributed on several hours before reaching the peak of intensity, the IWV fluctuates around maxima of about 60 kgm^{-2} when rainfall intensity registers 2.98 mmh^{-1} and 14.92 mmh^{-1}, respectively. Thus, during the precipitating phase, IWV drop down up to the minimum value around 20 kgm^{-2}. Unfortunately, only few hours are covered from the GPM-C overpasses. Although rain rates calculated from the 183-WSL is an instantaneous precipitation we found an overall agreement with raingauge measurements. The latter is particularly true for the first three events (Fig.2a, b and c) and the fifth (Fig.2e only at 1000 UTC) where lower precipitation regimes observed at ground are well reproduced by the 183-WSL retrievals.

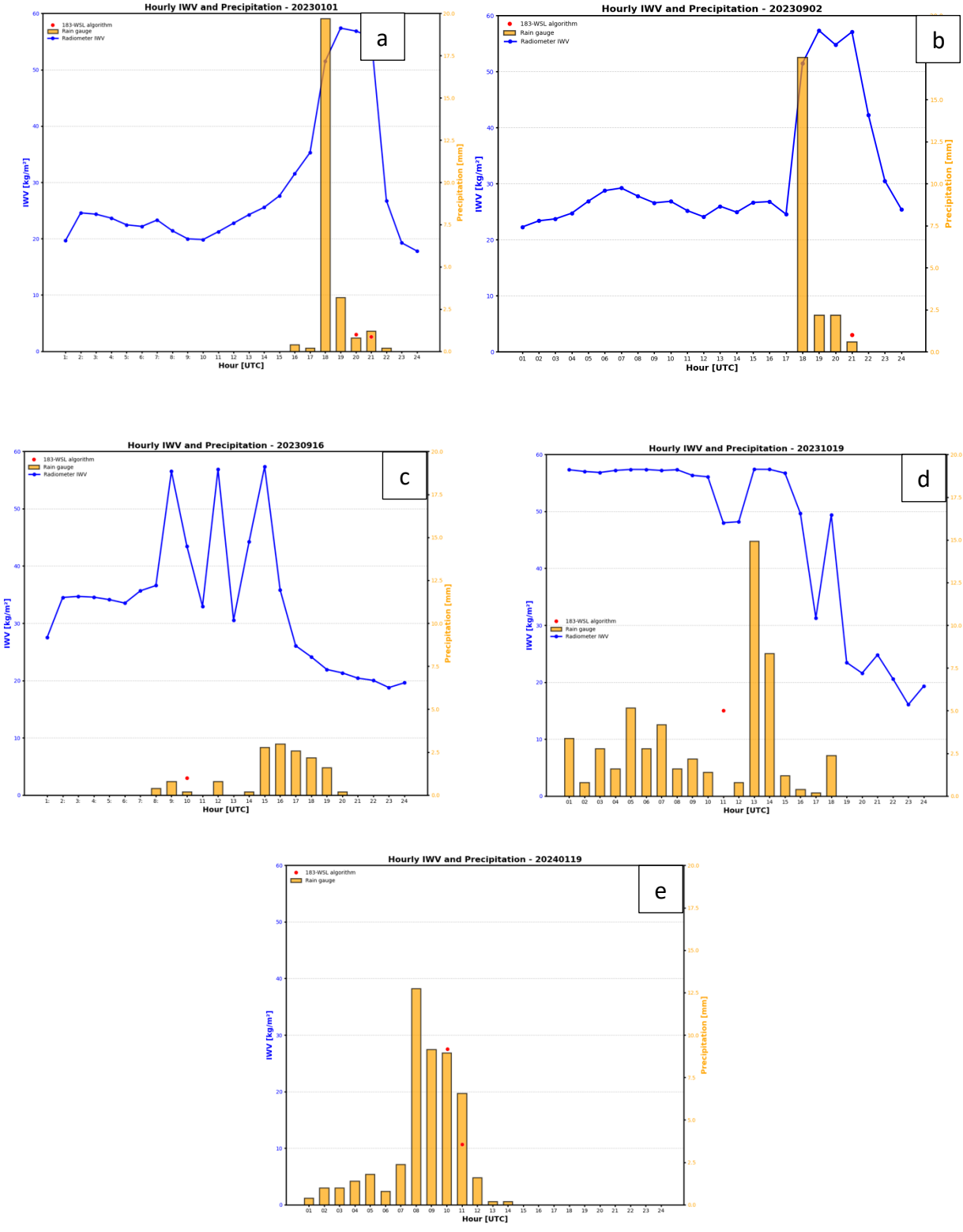

Fig. 2 – Bar diagrams to compare hourly rainfall, IWT and rain rate retrievals calculated from the 183-WSL (red dots). For diagram 2-e the IWV is missing.

4.1 Four-days variability of the atmospheric humidity

Although the results discussed in the previous section are quite rough due to the limited number of events, they were also used to further investigate the variability of atmospheric water vapor several hours before the precipitation begin. The scientific questions justifying this further investigation can be: how is the local distribution of the atmospheric water vapor before rain events? Can we delineate a tendency in the columnar water vapor to exploit it as a proxy variable to characterize the environment of the starting precipitation?
To do that, the Total Column Water Vapor (TCWV) available from ERA5 reanalysis has been used as a proxy variable. As observed in Fig.3 the distribution of TCWV is quite variable. However, a different behavior can be recognized.
The TCWV exponentially grows reaching the maximum value when precipitation intensity reaches the maximum as well. This is particularly true for short-time precipitation where the environmental conditions seem to be characterized by coupled behavior: several hours before rain the humidity tends to grow slowly as preparing the environment to accumulate humidity; few hours (less than 5 h) before rain, the atmospheric humidity steeply increase up to the peak of rain intensity. This condition can be observed in Fig.3a-b-c where short-time precipitating events are recorded. In the other two cases, where the precipitation is distributed in a longer time interval, the atmospheric humidity fluctuates during the rain event even though it shows a steep increase of rate by approaching the peak of intensity.
Although few cases were analyzed, we can conclude this section by asserting that the environmental conditions observed for the events in Fig.3a-b-c can favor the extreme precipitation, typically localized and associated to intense rain at ground. In the other cases (Fig.3d-e) we can say that the precipitation falling for an extended duration, usually characterized by low intensity regimes, is associated to a long-term fluctuation where the atmosphere follows a sequence of charge-discharge cycles of water vapor.

This effect is not unusual but the relationship between the increasing of the atmospheric water vapor and precipitation at ground can sustain new investigations in the perspective of the recent findings of increasing of the atmospheric humidity triggered by global warming.

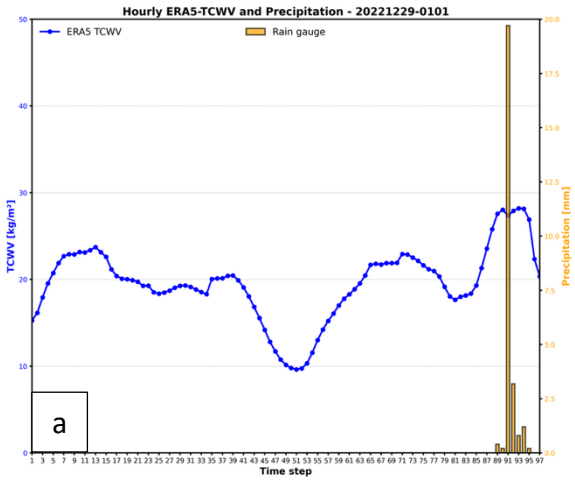

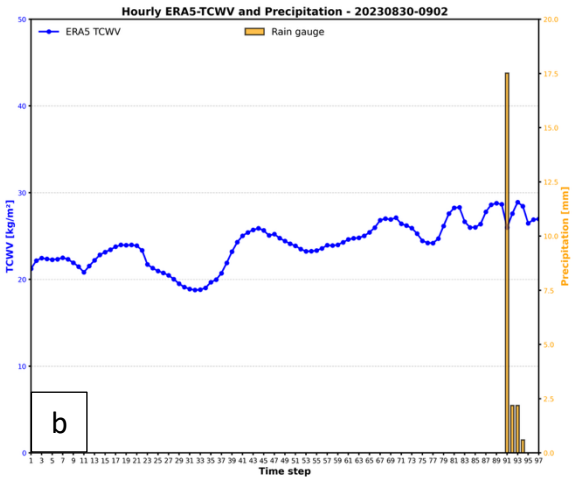

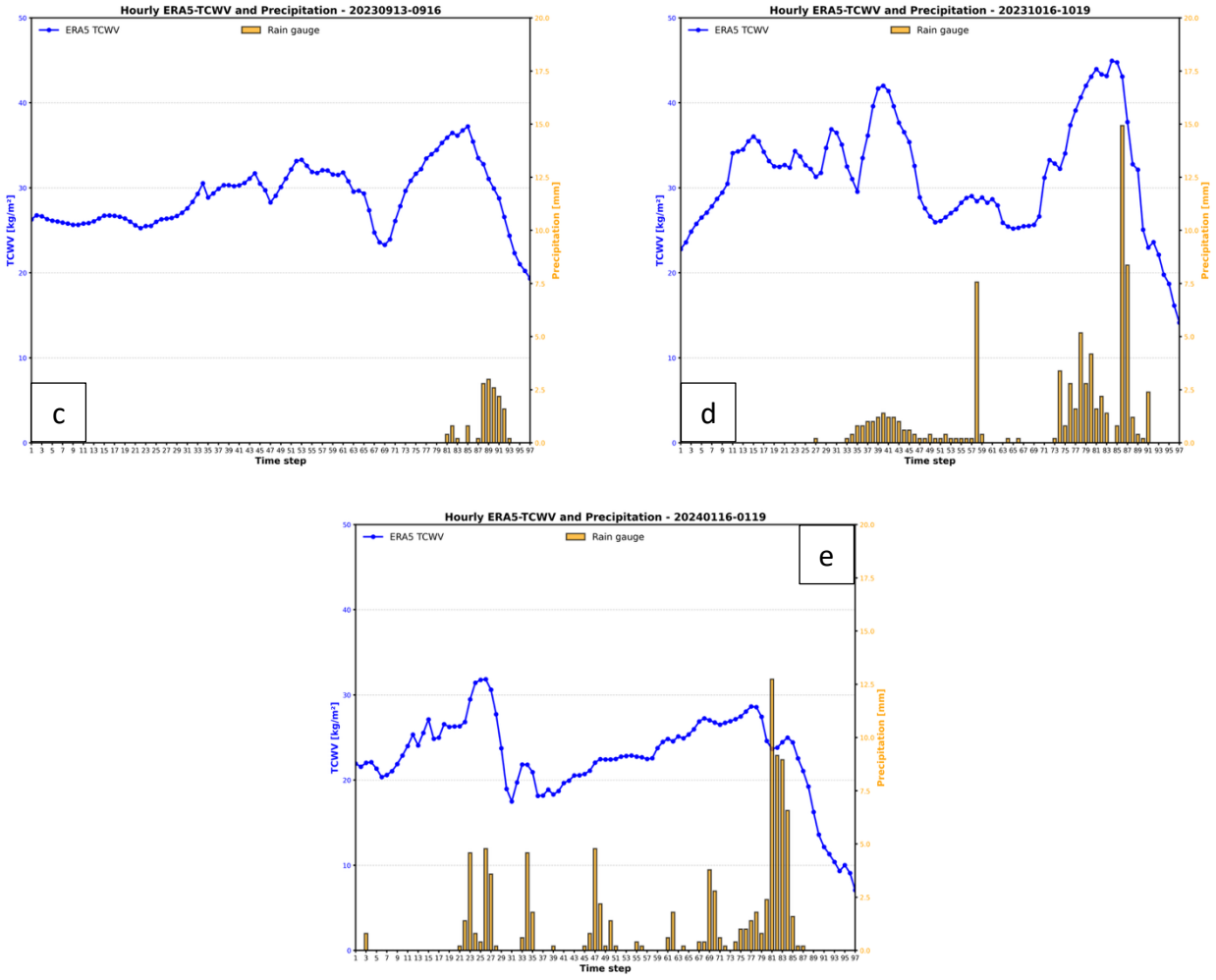

Fig. 3 – Comparison between hourly rainfall (bars) and TCWV from ERA5 reanalysis (blue line).

5. Conclusion and potential impacts

The results of this work contribute to answer the following scientific questions: 1) How do columnar water vapor change approaching precipitation? 2) Does water vapor constitute a good proxy to predict type of precipitation and the intensity of rain?

The high-resolution in-situ measurements of the MWR combined with raingauge hourly measurements and the retrievals of the 183-WSL method have improved the knowledge on the status of the atmosphere before, during and after a rain event. Under typical atmospheric conditions water vapor triggers, feeds and reinforces the precipitating systems. The heat lost by evaporation is carried deep into the atmosphere by convection and is released as heat by the atmosphere when water vapor condenses into rain.

The investigation of the amount of IWV temporally close to the rain events can sustain the practice of using water vapor measurement as a proxy variable for beginning rain. To corroborate and reinforce these results, the four-days distribution of columnar water vapor (TCWV) has been used. The using of TCWV as a proxy variable well delineated the behavior of the atmosphere to locally accumulate water vapor before rain. Several hours before rain the humidity tends to grow slowly as preparing the environment to progressively accumulate wet; few hours (less than 5 h) before rain, the atmospheric humidity steeply increases up to the peak of rain intensity.

The exploration of water vapor fluctuations close to rain events is also justified by the interest of the scientific community and needed of the operational and numerical meteorology increasingly prone to use satellite observations to link layered distribution of water vapor to weather phenomena.

References

Hou, A. Y., R. K. Kakar, S. Neeck, A. Azarbarzin, C. D. Kummerow, M. Kojima, R. Oki, K. Nakamura, and T. Iguchi, 2014: The Global Precipitation Measurement Mission. Bull. Amer. Meteor. Soc., 95, 701 722, doi:10.1175/BAMS-D-13-00164.1

Laviola S., V. Levizzani, E. Cattani, and C. Kidd, 2013: The 183-WSL fast rain rate retrieval algorithm. Part II: Validation using ground radar measurements. Atmos. Res., 134, 77-86, https://doi.org/10.1016/j.atmosres.2013.07.013

Laviola S., and V. Levizzani, 2011: The 183-WSL fast rain rate retrieval algorithm. Part I: Retrieval design. Atmos. Res., 99, 443-461, https://doi.org/10.1016/j.atmosres.2010.11.013

Laviola S., V. Levizzani, R. R. Ferraro, and J. Beauchamp, 2020a: Hailstorm detection by satellite microwave radiometers. Remote Sens., 12(4), 621; https://doi.org/10.3390/rs12040621

Laviola S., G. Monte, V. Levizzani, R. R. Ferraro, and J. Beauchamp, 2020b: A New Method for Hail Detection from the GPM Constellation: A Prospect for a Global Hailstorm Climatology. Remote Sens., 12(21), 3553; https://doi.org/10.3390/rs12213553

Rose T., S. Crewell, U. Löhnert, and C. Simmer, 2005: A network suitable microwave radiometer for operational monitoring of the cloudy atmosphere. Atmos. Res., 75, 183-200, doi:10.1016/j.atmosres.2004.12.005

Trenberth, K.E., P.D. Jones, P. Ambenje, R. Bojariu, D. Easterling, A. Klein Tank, D. Parker, F. Rahimzadeh, J.A. Renwick, M. Rusticucci, B. Soden and P. Zhai, 2007: Observations: Surface and Atmospheric Climate Change. In: Climate Change 2007: The Physical Science Basis. Contribution of Working Group I to the Fourth Assessment Report of the Intergovernmental Panel on Climate Change [Solomon, S., D. Qin, M. Manning, Z. Chen, M. Marquis, K.B. Averyt, M. Tignor and H.L. Miller (eds.)]. Cambridge University Press, Cambridge, United Kingdom and New York, NY, USA.

Vaquero-Martínez J., M. Antón, M. J. Costa, D. Bortoli, F. Navas-Guzmán, and L Alados-Arboledas, 2023: Microwave radiometer, sun-photometer and GNSS multi-comparison of integrated water vapor in Southwestern Europe. Atmos. Res., 287, 106698, https://doi.org/10.1016/j.atmosres.2023.106698

Acknowledgments

This work is performed in the context of the scientific cooperation of the Group of Satellite Meteorology at the CNR-ISAC and the Évora Atmospheric Sciences Observatory (EVASO) of the University of Évora in the ATMO-ACCESS TransNational Access project.